

Development of a model to identify local hydrogeology and
simulate groundwater injection in Nuuanu and Kalihi aquifer
systems, Oahu, Hawaii

A final report submitted to the graduate division of the University of Hawaii at
Manoa in partial fulfillment of the requirements for the degree of

Master of Science Plan B
in
Geology and Geophysics

December 2017

by
Brytne Okuhata

Committee:
Chair: Dr. Aly El-Kadi
Dr. Henrietta Dulai
Dr. Delwyn Oki
Dr. Bradley Carr

Table of Contents

Table of Contents	II
List of Figures	III
List of Tables	IV
Executive Summary	V
1. INTRODUCTION	7
2. DESCRIPTION OF STUDY AREA	9
2.1. Geology	9
2.1.1. <i>Koolau basalt</i>	9
2.1.2. <i>Alluvium</i>	10
2.1.3. <i>Honolulu volcanics</i>	10
2.1.4. <i>Caprock</i>	11
2.2. Hydraulic Properties	11
2.2.1. <i>Hydraulic Conductivity</i>	11
2.2.2. <i>Unsaturated zone parameters</i>	13
3. METHODS & MATERIALS	15
3.1. Groundwater model set-up	15
3.1.1. <i>Model framework and components</i>	16
3.1.2. <i>Boundary conditions</i>	19
3.1.3. <i>Inflow and outflow</i>	19
3.1.4. <i>Observation wells</i>	23
4. RESULTS & DISCUSSION	24
4.1. Model results	24
4.1.1. <i>Steady-state saturated flow calibration</i>	24
4.1.2. <i>Transient saturated flow calibration</i>	26
4.1.3. <i>Modeling well injection by use of saturated/unsaturated flow model</i>	29
5. SUMMARY AND CONCLUSIONS	33
Acknowledgements.....	35
References.....	36

List of Figures

Figure 1. Map of the study area, highlighting the Nuuanu and Kalihi aquifer systems, Nuuanu Reservoir No. 1 and Nuuanu Reservoir No. 4.....	9
Figure 2. Schematic diagram depicting procedures used to create a model for this study.	15
Figure 3. Numerical model mesh.	16
Figure 4. Conceptual model schematic.	17
Figure 5. Map of monitoring wells.	24
Figure 6. Results of saturated model calibration.....	25
Figure 7. Transient simulated head elevations plotted against transient observed head elevations and transient recharge from 2004 to 2014.....	28
Figure 8. Location of potential injection well against a Google Earth image (left) and the modeled mesh (right).....	29
Figure 9. Geologic cross-section through potential injection site.	30
Figure 10. Water table elevation along cross-sections A-A' and B-B' after 10 years of water injection simulation	31
Figure 11. Water table elevation after 10 years (top) and 25 years (bottom) of 4,315 m ³ /d water injection simulation.	32
Figure 12. Calculated capture zones of particles reaching Kalihi pump station..	33

List of Tables

Table 1. Previous estimates of hydraulic conductivities.....	13
Table 2. Aquifer parameter values used in the Nuuanu and Kalihi aquifer numerical model.	18
Table 3. Averaged water well pumping rates from the Nuuanu and Kalihi aquifers.....	22
Table 4. Observed water level data from the Nuuanu and Kalihi aquifers (2000-2017).	23

Executive Summary

Groundwater is the primary source of fresh drinking water for Hawaii's residents, but may be adversely affected by climate change. An overall decrease in groundwater recharge and an increase in population can negatively affect the state's fresh groundwater availability. It is therefore important to implement groundwater conservation measures to ensure that the islands have a stable source of groundwater for years to come. One potential approach is Aquifer Storage and Recovery (ASR), which involves harvesting fresh surface water and injecting the water into the subsurface aquifer. This study assesses the possibility of implementing ASR on the island of Oahu, Hawaii, for the Nuuanu and Kalihi aquifer systems. Surface water will be harvested from Nuuanu Reservoir No. 4 (NR4) and injected downstream near Nuuanu Reservoir No. 1 (NR1).

To assess the feasibility of the approach, the geologic subsurface of both aquifer systems was characterized with borehole logs and surficial geology maps and a numerical groundwater model was developed. The model was created using the groundwater numerical modeling software FEFLOW. The model was developed under steady-state, saturated conditions and calibrated using water levels from six observation wells. The calibration achieved a mean error (\bar{E}) of 0.71 m, a root mean square (RMS) of 0.80 m, and a standard deviation (1σ) of 0.88. The model was also calibrated with transient data to determine if the parameter values were acceptable. The model was further extended to account for unsaturated conditions to simulate water injection into the aquifer's unsaturated zone. A watershed modeling component estimated that surficial water can be harvested from NR4 at a maximum rate of 8,631 cubic meters per day (m^3/d). Such an amount was therefore simulated as the maximum anticipated injection rate to assess the aquifer's response under an extreme condition. A second simulation assessed half of the injection ($4,135 \text{ m}^3/\text{d}$) to further evaluate the aquifer response. According to regulatory conditions, water cannot be injected into the saturated zone. Therefore, the harvested water will likely need to be injected into the alluvium and Honolulu volcanics layers, at an elevation of 80 to 100 m, approximately 30 to 50 m below the ground surface. Based on the model results, the injected water body surrounds the injection well while percolating down to the saturated zone. However, the maximum injected water amount created a fully saturated mound above the water table as time progresses, violating regulatory conditions. It is recommended either to use a smaller injection rate or distribute the injected amount over a number of injection wells. No ground flooding is

expected to occur and the injection well potentially falls just within the 15-year capture zone of Kalihi pumping station.

The main limitation of this study includes the lack of borehole logs to validate the subsurface lithology and the lack of current data to calibrate the model. Though a general subsurface geologic model was created, it is still important to utilize future studies to validate the results to decipher the extreme subsurface heterogeneity. Future research should invest in borehole logs and geophysical investigations, specifically around NR1. The borehole logs will not only provide more insight into the geologic subsurface but will also be used to analyze hydraulic properties, such as hydraulic conductivity. Also, future research should obtain more current water level data covering the Nuuanu and Kalihi aquifer systems. Other natural tracer data, such as temperature, can be useful in model calibration.

1. INTRODUCTION

Groundwater is a crucial freshwater resource for Hawaii, as is the case for island nations. However, such a resource within volcanic island aquifers may be adversely affected by climate change and anthropogenic activity (Izuka et al., 2016). Since the Hawaiian Islands are relatively small, volcanic aquifers have a limited groundwater storage capacity. Furthermore, the islands' coasts are completely surrounded by salt water and majority of the fresh groundwater sits upon the denser salt water (Izuka et al., 2016). Nonetheless, approximately 99% of Hawaii's domestic freshwater is pumped from the groundwater aquifers (Gingerich and Oki, 2000). Although pumping rates are less than 3% of the average rainfall rate, water shortages can still occur due to the uneven rainfall spatial distribution and to the fact that a large portion of rainfall flows to the ocean via streams and returns back to the atmosphere via evapotranspiration (Gingerich and Oki, 2000). Therefore, water conservation approaches naturally emphasize methods to reduce these losses.

Decrease in recharge and increase in groundwater withdrawal are the major factors that can affect Hawaii's future fresh groundwater availability. Annual rainfall trends have been declining since 1920, resulting in drought conditions across the state, particularly on the leeward side of the islands (Diaz and Giambelluca, 2012; Frazier and Giambelluca, 2016). Such sides of the islands show a drying trend during dry seasons, especially on the islands of Oahu and Maui (Timm et al., 2015). Rainfall trends on the windward sides of the islands, however, are expected to maintain or slightly increase during wet seasons (Timm et al., 2015). The overall declining rainfall trend reduces the volume of water able to reach the groundwater aquifer, thus reducing the availability of fresh groundwater (Chu and Chen, 2005; Timm et al., 2015). Human activity can also negatively impact the islands' fresh groundwater availability. With a growing population, pumping rates will inevitably increase in order to meet water demands. Oahu, the most densely populated island in Hawaii, is home to 953,207 people, which is approximately 70% of the state's population (U.S. Census Bureau, 2011). Groundwater withdrawals on Oahu averaged about 791,000 cubic meters of water per day from 2000 to 2010 (Izuka et al., 2016). Withdrawal of fresh groundwater can lead to saltwater intrusion which affects the quality of water pumped by wells (Izuka et al., 2016). This was seen in the late 1900s, when withdrawals

and free-flowing artesian wells caused the freshwater head in southern Oahu to drop from 13 meters to 8 meters above mean sea level (Takasaki, 1978). In this situation, well water, which was initially fresh and of potable quality, became brackish over a 50-year span (Takasaki, 1978). Thus, increased pumping can result in a depletion of fresh groundwater.

It is important to implement water conservation and water resource management strategies in order to enhance Oahu's future fresh groundwater availability. Potential water conservation strategies include Aquifer Storage and Recovery (ASR), which involves harvesting surface water and injecting the water into the aquifer system. The injected water recharges the groundwater aquifer and can be recovered from nearby pumping wells (EPA, 2016). This ASR method is widely used in the western and southeastern regions of the U.S., as well as in seven other countries (Pyne, 2003; EPA, 2016), including South Korea (Kim et al., 2008) and South Australia (Martin and Dillion, 2002). Surface water is ideally harvested from wet areas of the island during the wet season, and recovered during the dry season, when water demands are higher (Pyne, 2003).

The Nuuanu and Kalihi aquifer systems are potential areas to implement the ASR method. A 20-meter-high dam was constructed between 1905 and 1910 to create Nuuanu Reservoir No. 4, located atop the Nuuanu and Kalihi aquifer systems (Star Bulletin, 2006; RM Towill Corporation, 2013). By 1919, surface water from the reservoir was no longer required as a potable water source because artesian wells were constructed in Honolulu (RM Towill Corporation, 2013). Today, approximately 303,000 cubic meters of water is stored in the reservoir, but is not in use (Star Bulletin, 2006). The surface water stored in NR4 can be harvested and injected near Nuuanu Reservoir No. 1 (NR1), which is located downstream of NR4. Since Honolulu is the most densely populated city on Oahu, NR4 and NR1 are excellent locations to implement the ASR method.

The three primary objectives of this study were to (1) identify the local and regional lithology and hydrological parameters of the Nuuanu and Kalihi aquifer systems, (2) evaluate a possible injection well location and depth near NR1, and (3) assess the response of the aquifers to the harvested freshwater injection through the use of groundwater and particle tracking models.

2. DESCRIPTION OF STUDY AREA

This research models the Nuuanu and Kalihi aquifer systems (Fig. 1), which make up part of the Honolulu watershed, located on the south side of the island of Oahu (Wentworth, 1941). The model covers the leeward slopes of the mountain, spanning from the ridge of the Koolau Range down to the coastline and offshore. The Nuuanu and Kalihi aquifer systems have an area of approximately 38.3 km² and 25.5 km², respectively. The aquifer systems comprise four primary geologic formations: Koolau basalt, alluvium, Honolulu volcanics, and caprock.

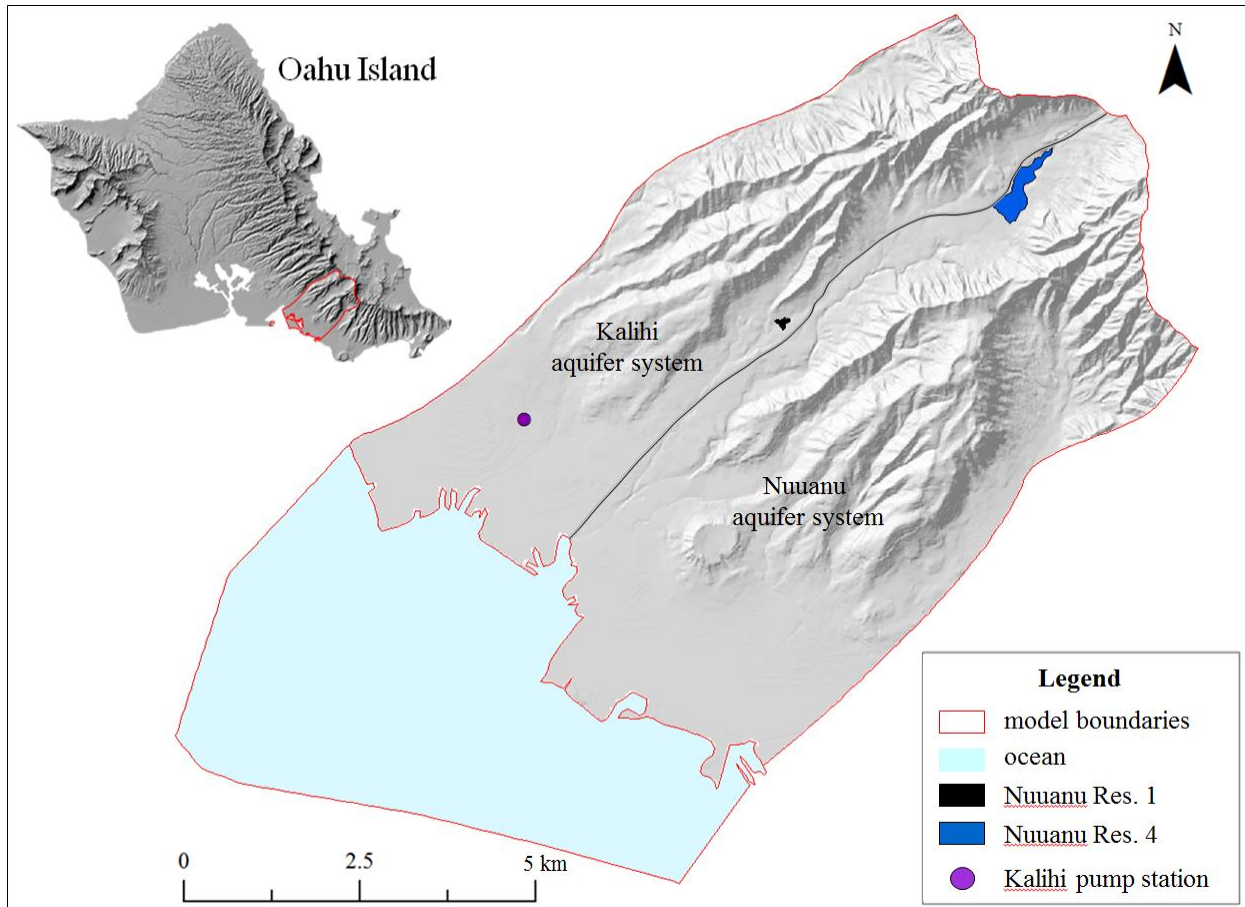


Figure 1. Map of the study area, highlighting the Nuuanu and Kalihi aquifer systems, Nuuanu Reservoir No. 1 and Nuuanu Reservoir No. 4.

2.1. Geology

2.1.1. Koolau basalt

The Koolau basalt, a shield-stage tholeiitic basalt, forms the bulk of the Koolau Range, including the Nuuanu and Kalihi aquifer systems. The Koolau basalt lava flows are typically thinly bedded,

ranging from 3 to 24 meters in thickness. It is believed that the Koolau basalt flowed in rapid succession due to the lack of erosional unconformities and soil beds (Stearns and Vaksvik, 1935; Palmer, 1946; Wentworth, 1951). The Koolau basalt flowed both as pahoehoe and aa lava flows. The lava flows contain a wide variety of void spaces, including intercrystal spaces, shrinkage cracks, gas pores, clinker voids, bedding voids, and lava tubes (Palmer, 1946). These features allow the Koolau basalt to act as an excellent water-bearing aquifer.

2.1.2. Alluvium

Once lava extrusion from the Koolau volcano stopped, streams eroded the Koolau basalt to create deep valley incisions. The erosion process occurred continuously until the valleys were incised to their current width, when precipitation and drainage area were reduced (Stearns and Vaksvik, 1935). Following the erosion, the island subsided approximately 2,000 to 4,000 meters (Stearns and Vaksvik, 1935; Moore, 1987). These events resulted in aggradation, in which alluvium (also referred to as “valley fill”) filled the floors of the incised valleys (Stearns and Vaksvik, 1935). Diamond drillings and well borings strongly suggest that the alluvium continuously overlays the entire width and most of the length of the valley floors (Wentworth, 1941). Since the island had subsided prior to the alluvium deposition, much of the alluvium at lower elevations was deposited when sea level was lower than the current sea level. Therefore, the contact between alluvium and underlying Koolau basalt lies below the current water table elevation in areas of relatively lower elevation (Rotzoll and El-Kadi, 2007; Izuka et al., 2016).

2.1.3. Honolulu volcanics

Following erosion and sediment deposition, rejuvenation-stage volcanism occurred within the Pleistocene epoch (Wentworth, 1951). During this time, the Honolulu volcanics were layered on top of the alluvium, within the eroded valleys (Stearns and Vaksvik, 1935). The Honolulu volcanics differ greatly from the Koolau basalt, consisting primarily of alkalic, nepheline, and nepheline-melilite basalts (Wentworth, 1951). Since the Honolulu volcanics were deposited after the severe weathering and erosion, the Honolulu volcanics are disconnected from the Koolau basalt and basal water system (Wentworth, 1941).

2.1.4. Caprock

Coastal-plain deposits lie on top of the alluvium and volcanics to form a semiconfining unit called the caprock (Oki, 2005; Izuka et al., 2016). The caprock is comprised of marine sediments and reef limestone, as well as terrestrial sediments accumulated from the Koolau basalt and Honolulu volcanics. Towards the eastern coast near Waikiki, the caprock extends a little over a mile inland, while the caprock extends at least three miles inland towards the western coast near Moanalua (Palmer, 1946). The caprock can be up to 480 meters thick offshore. The caprock is a crucial part of the Nuuanu and Kalihi aquifer systems because, as a semiconfining layer, it greatly retards the outflow of groundwater from the permeable Koolau basalt. Therefore, the caprock allows the aquifers to accumulate fresh groundwater and artesian sources (Izuka et al., 2016). The upper portion of the caprock is primarily composed of reef limestone, which is atypical of the general caprock unit. Since the upper limestone is unconfined and highly permeable, it is a good source for brackish groundwater, which can be pumped for irrigation and/or cooling purposes (Oki, 1996). Lagoonal deposits reside as a relatively thin layer on top of the upper limestone along the coast line. The lagoonal deposits typically have a lower permeability, thus retarding water drainage close to the shore (Finstick, 1998).

2.2. Hydraulic Properties

The hydraulic properties of different geologic units can drastically alter the flow of groundwater within an aquifer system. The following hydraulic properties were crucial parameters considered while modeling the Nuuanu and Kalihi aquifer systems.

2.2.1. Hydraulic Conductivity

Hydraulic conductivity can be estimated based on Darcy's law:

$$q = -K \frac{dh}{dl} \quad (1)$$

where

q = specific discharge [L/T],
 K = hydraulic conductivity [L/T], and
 dh/dl = hydraulic gradient [L/L].

The hydraulic conductivity of lava flows is typically anisotropic, where the horizontal hydraulic conductivity (K_h) is usually much greater than the vertical hydraulic conductivity (K_v). For modeling purposes, Souza and Voss (1987) estimated a 200 to 1 ratio between K_h and K_v . The Koolau basalt has a relatively high hydraulic conductivity due to the joints and open spaces formed parallel to flow directions (Wentworth, 1951). These characteristics allow the Koolau basalt to store and transport most of the freshwater throughout the aquifer systems. Almost all artesian wells and municipal pumping wells are supplied by the Koolau basalt (Stearns and Vaksvik, 1935). Since the Koolau basalt is heterogeneously formed by thin lava flows, its hydraulic conductivity can vary drastically depending on its age, location, and exposure.

Due to extensive weathering, alluvium has a lower hydraulic conductivity than the Koolau Basalt (Lau and Mink, 2006). Therefore, alluvium acts as a barrier retarding groundwater flow to the underlying aquifer (Rotzoll and El-Kadi, 2007). The Honolulu volcanics also have varying hydraulic conductivities due to the different rock types and conditions found interlayered within the volcanics. The Honolulu volcanics can contain units of cinders, ash, and weathered rocks, which alter the hydraulic conductivity of the material (Izuka et al., 2016). The caprock is comprised of different types of materials, thus its hydraulic conductivity can vary drastically. The lower caprock contains more clay and mud, thus it has a relatively low hydraulic conductivity, typically less than 0.3 m/d, and impedes the outward flow of freshwater (Izuka et al., 2016). In comparison, the caprock's upper limestone unit has a relatively high hydraulic conductivity, and can even exceed the hydraulic conductivity of lava flows. Previously estimated hydraulic conductivity values for these geologic units can be found in Table 1.

Table 1. Previous estimates of hydraulic conductivities.

Geologic unit	Hydraulic conductivity range (m/d)	Area	Reference
	150 – 1500	Oahu island	Hunt, 1996
	460	downtown Honolulu	Finstick, 1998
Koolau basalt	350 – 1700	Ewa	Oki, 1998
(dike-free lava)	550 – 1100	Palolo-Waiialae	Lau & Mink, 2006
	150 – 1500	South Oahu	Souza & Voss, 1987
marginal dike zone	30 – 310	Oahu island	Hunt, 1996
	0.3 – 150	Oahu island	Hunt, 1996
Alluvium	0.01 – 0.11	Palolo-Waiialae	Lau & Mink, 2006
	0.9	downtown Honolulu	Finstick, 1998
	0.0035 – 0.35	Ewa	Oki, 1998
Honolulu volcanics	0.3 – 150	Oahu island	Hunt, 1996
	0.003 – 0.3	Palolo-Waiialae	Wentworth, 1938
caprock	0.01 – 100	Pearl Harbor	Souza & Voss, 1987
	31	downtown Honolulu	Finstick, 1998
	1 – 780	Waikiki	Habel et al., 2017
upper limestone	30 – 6000	Oahu island	Hunt, 1996
	0.43 – 53	downtown Honolulu	Finstick, 1998
lagoonal deposits	0.5 – 1	downtown Honolulu	Finstick, 1998

2.2.2. *Unsaturated zone parameters*

In this study, harvested water will be injected in the unsaturated zone, which lies between the ground surface and the water table. The pore spaces of such a zone, consisting of soil, saprolite, and rocks, contain both water and air, in contrast to the saturated zone where pores are completely filled with water (Gingerich and Oki, 2000; Lau and Mink, 2006).

Hydraulic parameters of the unsaturated zone are not well quantified for deep formations existing in Hawaii. In addition, the governing equation representing groundwater flow is non-linear in nature, thus making it difficult to model. Nonetheless, the unsaturated zone is an important part of the aquifer system because it controls the pathway transmission of surface water to the deep aquifers (Hunt et al., 1988). Two fundamental parameters to consider while modeling the unsaturated zone are water content (θ) and matric pressure (ψ). Water content is defined as the volume of contained water per total volume of medium (Fetter, 2001; Nimmo, 2009). Matric pressure (also referred to as moisture potential and soil capillary head) is the negative pressure caused by the attraction between soil and water (Fetter, 2001). If a medium has high ψ , that medium has drier pore space, therefore more potential to be filled with water. Thus, ψ and θ are inversely related (Fetter, 2001).

The rate of water flow through an unsaturated medium is dependent upon the unsaturated hydraulic conductivity, which is dependent upon θ . As pores fill with water, thus increasing θ , the hydraulic conductivity also increases (Fetter, 2001). The relationship between θ , ψ , and hydraulic conductivity can be represented by a water retention curve (WRC). Curve fitting models, such as the semi-empirical model of van Genuchten (1980), are used to characterize the relationship between both hydraulic conductivity and θ versus ψ . The van Genuchten model is defined as:

$$S_e = \frac{(\theta - \theta_r)}{(\theta_s - \theta_r)} = \frac{1}{[1 + (\alpha\psi)^n]^m} \quad (2)$$

where

- S_e = effective saturation,
- θ = water content [L^3/L^3],
- θ_r = residual water content,
- θ_s = saturated water content,
- ψ = matric pressure [kPa],
- α = empirical parameter [kPa^{-1}],
- n = empirical parameter [dimensionless], and
- m = empirical parameter ($m=1-1/n$).

The saturated water content (θ_s) is the maximum volume of water a medium can hold, thus generally equated to porosity. Parameter α is related to the air-entry value of soil and n is a measure of the pore-size distribution (Fredlund and Xing, 1994). The model also provides an expression for the unsaturated conductivity function $K(S_e)$.

3. METHODS & MATERIALS

3.1. Groundwater model set-up

To assess the response of the Nuuanu and Kalihi aquifer systems to freshwater injection, this study used various geologic and observation data sets to develop a three-dimensional groundwater model (Fig. 2). The Groundwater Modeling System (GMS) (<http://www.aquaveo.com>) was utilized in creating the site's conceptual model and FEFLOW (<https://www.mikepoweredbydhi.com/>) was used in the model development. FEFLOW was used to simulate groundwater flow and particle transport within Nuuanu and Kalihi aquifer systems, and in evaluating the effect of freshwater injection on the aquifers.

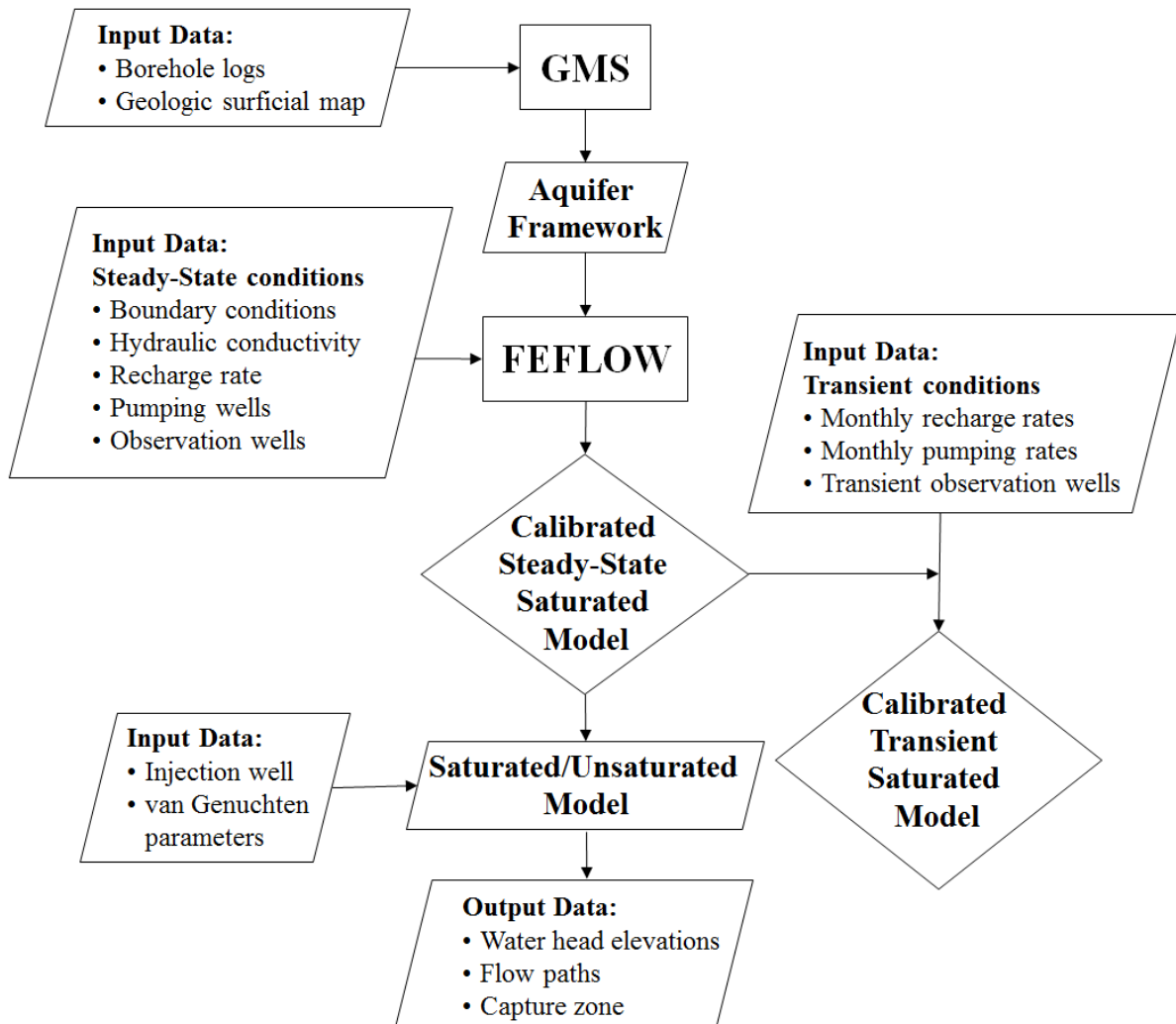


Figure 2. Schematic diagram depicting procedures used to create a model for this study.

3.1.1. Model framework and components

The model consists of 15 layers, which are each made of 12,227 triangular elements, totaling 183,405 elements (Fig. 3). The upper surface of the model is characterized by LiDAR topographic digital elevation maps (DEMs) (NOAA, 2007). Only freshwater was simulated by setting the bottom elevation of the model as the freshwater – saltwater interface, calculated from the Ghyben-Herzberg principle (Fetter, 2001) (Fig. 3b). Such an assumption was also adopted by Whittier et al. (2010). It is however important to note that unlike the model created by Whittier et al. (2010), this model extends past the shoreline, therefore such an assumption may not realistically apply. This limitation can be addressed with a future density-dependent model. The finite elements vary in size due to mesh refinement around the pumping wells. The model extends from the marginal dike zone along the Koolau Ridge to approximately 3.1 ± 1.1 km offshore. This offshore portion was included in order to model the occurrence of fresh groundwater discharge within the coastal ocean area.

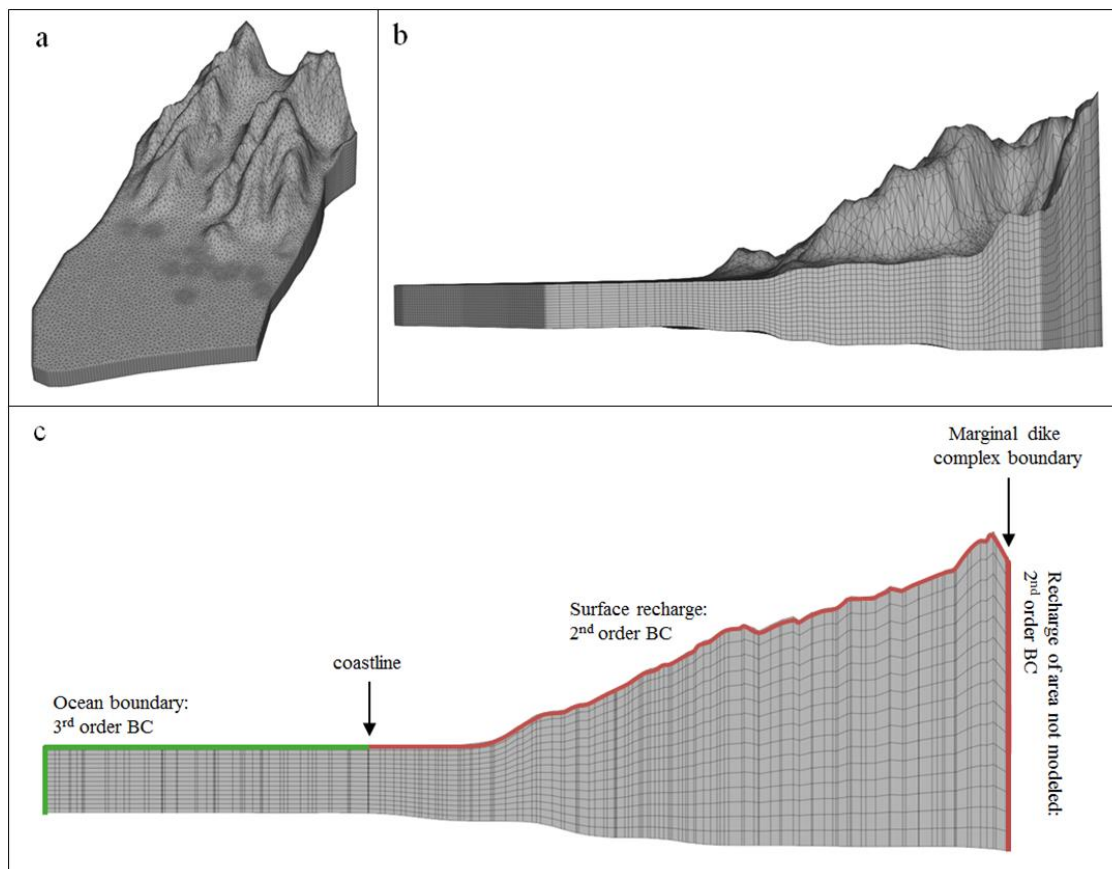


Figure 3. Numerical model mesh. (a) Bird’s eye view of model, including mesh refinement around pumping wells. (b) Side view of layered mesh, where the bottom of the model follows the estimated freshwater-salt water interface. (c) Cross-section showing boundary condition distributions.

The conceptual lithologic layering was created using borehole logs and a surficial geologic map (Fig. 4). Wentworth (1941) documented 12 borehole logs and constructed two cross-sections from the upper Nuuanu Valley. These logs and cross-sections approximated the dimensions of the various lithologic layers constructed for this model. The logs and cross-sections confirm a layer of alluvium that blankets the Koolau basalt across the entire width of Nuuanu Valley, extending approximately 130 m below the valley floor. Numerous layers of Honolulu volcanics cover the alluvium, reaching a thickness of approximately 100 m in the upper valley. Two logs from wells (1752-01, 1752-02) located in the coastal plain of the Nuuanu aquifer system and one log from well 2050-01 within Nuuanu Valley was obtained from the Honolulu Board of Water Supply (HBWS) (Fig. 4). These logs indicated that at lower elevations, the Honolulu volcanics and alluvial layers extend approximately 20 m below mean sea level. The bottom elevation of the caprock was determined using data from Rotzoll and El-Kadi (2007).

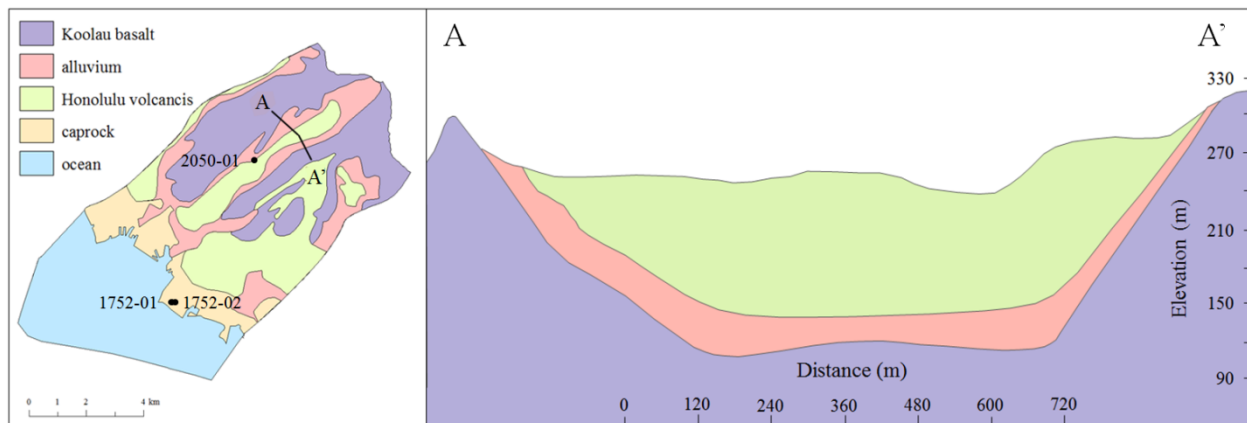


Figure 4. Conceptual model schematic. (left) Surficial geologic map modified from (Sherrod et al., 2007). (right) Conceptual cross-section through upper Nuuanu Valley modified from Wentworth (1941).

Hydraulic conductivity (K) values were assigned to each lithologic unit (Table 2). The horizontal longitudinal K values were estimated based on previously determined values (Table 1) and parameter estimation. As previously determined by Souza and Voss (1987), horizontal K values for the basalt aquifer are approximately 200 times greater than the vertical K values. Since the alluvium, caprock, upper limestone, and lagoonal deposits were not deposited in the same manner as the lava flows, the contrast between horizontal and vertical K values are not as severe.

Table 2. Aquifer parameter values used in the numerical model.

Material	hydraulic conductivity (m/d)			conductance (1/d)	porosity & specific yield	
	horizontal (longitudinal)	horizontal (transverse)	vertical		scenario 1	scenario 2
Koolau basalt	600	150	0.75		0.08	0.3
Alluvium	0.05	0.05	0.05		0.3	0.5
Honolulu volc.	3	1	0.03		0.1	0.1
Caprock	1×10^{-6}	1×10^{-6}	1×10^{-6}	1×10^{-8}	0.1	0.1
Upper limestone	100	100	0.5	1	0.2	0.2
Lagoonal deposit	1	1	0.5		0.1	0.1

The assigned hydraulic conductivities were used to calculate the conductance of each material. Conductance was defined as:

$$\Phi = K/d \quad (3)$$

where

K = hydraulic conductivity [L/T] and

d = layer thickness [L].

Conductance was assigned to lithologic units associated with a fluid-transfer boundary condition (further discussed in section 3.1.2). The conductance of each material was set as an inflow/outflow transfer rate for head-dependent flow boundary conditions.

Specific yield and porosity values were treated as equal and estimated based on values computed by Wentworth (1938) and used by Oki (2005). Specific yield values were assigned to the transient model and porosity values were assigned to the saturated/unsaturated model (further discussed in section 4.1.3.). Wentworth (1938) measured porosity values for Koolau basalt from 0.05 to 0.51 and measured porosity values for Honolulu volcanics from 0.01 to 0.16. Oki (2005) assigned the upper limestone unit a porosity value of 0.2 and all other rocks that were not considered part of the volcanic-rock aquifer a porosity value of 0.1. For this model, two specific yield and porosity scenarios were tested for calibration. In scenario one, Koolau basalt was assigned a porosity of 0.08, alluvium was assigned a porosity of 0.3, the upper limestone was assigned a porosity of 0.2, and all other rocks were assigned a porosity of 0.1 (Table 2). In

scenario two, Koolau basalt was assigned a porosity of 0.3, alluvium was assigned a porosity of 0.5, the upper limestone was assigned a porosity 0.2, and all other rocks were assigned a porosity of 0.1 (Table 2).

3.1.2. Boundary conditions

The top of the caprock beyond the coastline (below mean sea level) was set as a zero meter fluid-transfer boundary condition. Such a condition is a third-order Cauchy type, where the flux is dependent upon a pre-defined reference head and the material conductance. The top of the model and the northeast vertical boundary were treated as a fluid-flux boundary condition, or a second-order Neumann condition, where the flux across the boundary is specified. This boundary condition will be further discussed in section 3.2.3. The southeast and northwest boundaries were treated as no-flow boundaries. Since these boundaries fall along Kalihi stream and Manoa stream valleys, the less permeable valley fill may act as a barrier preventing groundwater flow across aquifers (Oki, 1998; Oki, 2005).

3.1.3. Inflow and outflow

Recharge data (inflow) for the Nuuanu and Kalihi aquifer systems were obtained from an Oahu Island water budget (Engott et al., 2015). This water budget was calculated based on 1978 to 2007 rainfall data, 2010 land cover data, and average climate conditions. The original recharge coverage does not account for interactions between surface water and groundwater, thus baseflow was not fully removed from the coverage; baseflow was only removed from direct runoff calculations. Therefore, we calculated baseflow and removed it from the original coverage in order to apply it to this research model. The baseflow was calculated with data from three stream stations (Nuuanu: 16232000, Waiakeakua: 16240500, Kalihi: 16229300) across the aquifers using the USGS Groundwater Toolbox. The baseflow values were removed from the corresponding drainage basin areas, which were calculated using the USGS StreamStats application. Since it is not appropriate to apply a baseflow value to the drainage basin downstream of a stream station, baseflow was only calculated and removed from the areas upstream of the stations. The total recharge volume before baseflow removal was approximately 111,000 m³/d, which was reduced to approximately 92,000 m³/d after baseflow was removed. A transient recharge coverage was obtained from a Nuuanu area watershed water budget which used the soil and water assessment tool (SWAT) to calculate transient rates (Leta et al., 2017).

These authors calculated monthly recharge rates between 2004 and 2014. Their water budget separates out a component called lateral flow from the groundwater recharge calculation. The lateral flow represents subsurface flow from the unsaturated area above the water table, which eventually reaches the stream. The water budget model used by Engott et al. (2015) does not separate the lateral flow component, thus likely includes it as groundwater recharge. Leta et al., however, assume that lateral recharge discharges to the streams, thus removes it from the estimated groundwater recharge. Therefore, it is important to add lateral flow to recharge computed by Leta et al. (2017) in order to properly compare to the recharge coverage created by Engott et al. (2015). The SWAT model computed a baseflow component, which was not initially removed from the recharge coverage computed by Leta et al. (2017). Therefore, the baseflow component computed by the SWAT model was removed from the recharge coverage, resulting in an average recharge volume of 108,000 m³/d from Leta et al. (2017). This final coverage, where lateral flow was added and baseflow was removed from recharge, was used for the transient model.

Since the model only extends to the marginal dike zone, the recharge located between the marginal dike zone and topographic divide (mountain ridgeline) was applied to the inland vertical boundary of the model. Since rainfall is highest between the marginal dike zone and the topographic divide, it is important that this area's recharge is not omitted from the model. Therefore, the recharge within this area was applied horizontally into the vertical boundary. A recharge rate of 0.01 m/d was applied to the upper vertical boundary to recover the recharge volume from the marginal dike zone. The rates applied to the top layer of the model and the rate applied to the upper vertical boundary of the model produced approximately 104,000 m³/d of groundwater recharge within the domain. This volume of 104,000 m³/d was the total recharge volume applied to the saturated, steady-state model. All of the recharge inflow was treated as a fluid-flux boundary condition during steady-state conditions. During transient conditions, FEFLOW has the option to apply recharge as a fluid-flow material property. Due to the fact that the transient recharge coverage contains a different shapefile for each month over the span of eleven years, it was more effective to assign the recharge as a material property rather than a boundary condition. Therefore, the top layer of the model was set as a fluid-flow material property (In/outflow at top/bottom), which computes net infiltration and allows for transient

fluxes. The horizontal inflow at the vertical boundary still remained as a rate of 0.01 m/d, so was kept as a fluid-flux boundary condition.

Pumping well data (outflow) were obtained from the Department of Land and Natural Resources (DLNR) Commission on Water Resource Management (CWRM). Twenty-two public and private wells throughout Nuuanu and Kalihi aquifer systems are currently being pumped and reported to CWRM. These wells include three primary pumping wells (Kalihi pumping station, Beretania pumping station, and Wilder Avenue well 3), which provide freshwater to the majority of Honolulu. This list may not include smaller privately owned wells, which are not being reported by the well owners. Pumping rates from 2002 to 2016 were obtained and averaged for each well (Table 3). The averaged pumping rate values were used for steady-state calibration and the monthly pumping rate values were used for transient calibration.

Table 3. Averaged water well pumping rates from the Nuuanu and Kalihi aquifer systems (2002-2016).

Well number	Top Screen Elevation (m)	Bottom Screen Elevation (m)	Pumping Rate (m ³ /d)
1750-09	-5	-14	760.9
1750-12	-5	-14	866.9
1752-01	-28	-226	2657.4
1752-02	-28	-226	10292.5
1849-10	-49	-85	580.5
1849-13	-92	-129	23897.2
1850-29	-11	-17	431.5
1851-07	-143	-162	18.9
1851-12	-146	-170	23299.2
1851-54	-98	-130	859.3
1851-62	-5	-17	3838.4
1851-68	-5	-17	5333.7
1851-73	-212	-233	140.1
1947-02	220	180	643.5
1948-01	-30	-122	1013.2
1952-06	-134	-150	19812.8
1952-15	-53	-94	3.8
2050-01	-2	-69	359.6
2051-01	-17	-48	249.8
2051-02	-15	-46	605.7
2052-13	-15	-46	4557.6
2052-14	-15	-46	2335.6

Top and bottom screen elevations are relative to mean sea level.

3.1.4. Observation wells

Observed water head levels were collected from CWRM, HBWS, and the U.S. Geological Survey (USGS) National Water Information System (NWIS) Mapper (<https://maps.waterdata.usgs.gov/mapper/index.html>). The observation data spans all the way back to the 1800s, but only observed water levels from 2000 to 2017 were considered for this study (Table 4). Water levels from the same well can drastically differ during different years, so it is not appropriate to calibrate the models with water level values that are not representative of current conditions. Only three wells have measured water levels between 2016 and 2017, so the time range was expanded to 2000 in order to calibrate more observation points. Those three wells (1952-06-08, 2052-10, and 1851-02) have continuous monitoring data, which were also used for the transient model calibration (Fig. 5).

Table 4. Observed water level data from the Nuuanu and Kalihi aquifers (2000-2017).

Well number	Year observed	Observed water level (m)	Source
1849-16	2000	6.4	NWIS
1851-54	2000	6.7	NWIS
2051-02	2000	6.7	NWIS
1952-06-08 *	2016	6.9	HBWS
2052-10 *	2017	7.0	HBWS
1851-02 *	2017	7.3	HBWS

Note: Wells marked with * have transient observation data, but the observed water level data listed represents a single level measurement during the indicated year. These levels were used for steady-state model. All observation wells are mapped in Fig. 5.

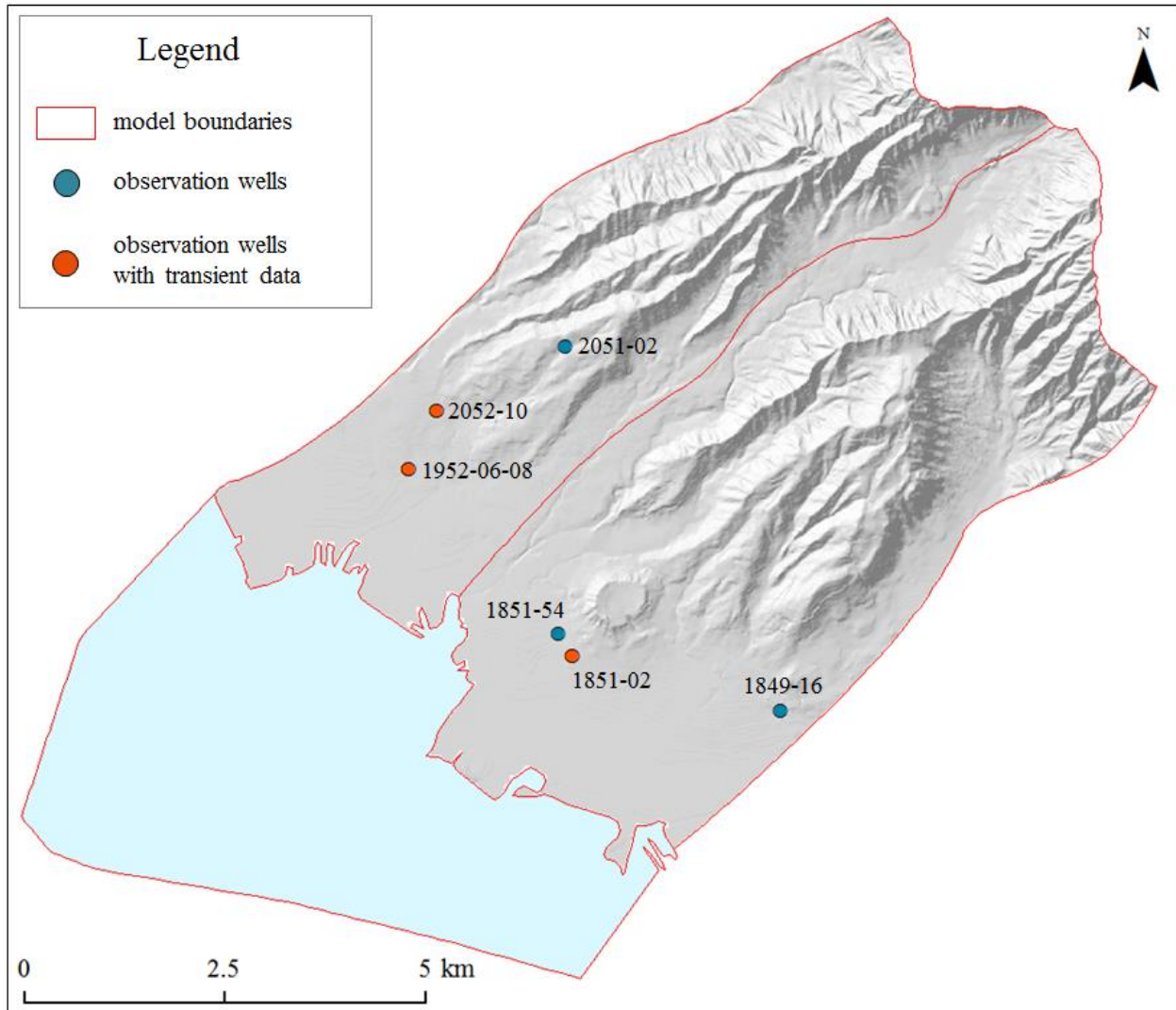


Figure 5. Map of monitoring wells. Observation well data can be found in Table 4.

4. RESULTS & DISCUSSION

4.1. Model results

4.1.1. Steady-state saturated flow calibration

The model was first calibrated under a saturated condition that ignored flow in the unsaturated zone and assumes a steady-state condition. The hydraulic conductivities were initially refined based on previously determined values (Table 1), then calibrated based on the six observed head levels (Table 4). Calibration was achieved with mean error (\bar{E}) of 0.71 m, root mean square (RMS) of 0.80 m, and standard deviation (1σ) of 0.88 (Fig. 6). Unfortunately, there was a lack of

spatial variation in heads amongst the observation points. There are no monitoring wells further inland of the aquifer, so it is uncertain how the computed head levels compare to the actual head levels at higher elevations. There was also a lack of current observation data which could be collected. Most of the observed water levels fell between six to seven meters head, yet the wells were distributed across the aquifers. This made it difficult to model an appropriate head gradient that would match every observed point. As seen in Fig. 6, the mauka (upland) simulated well head level was too high and the makai (seaward) simulated well head levels were too low. This however, resulted in accurate calibration of the wells that were centrally distributed. Although the model results are not as statistically significant as desired, the modeled head levels and gradient follow the overall distribution of observation points and generally match previously modeled results. Quantitatively validating the results against other models' results is difficult because other models focus in general on just basalt as the primary unit holding groundwater.

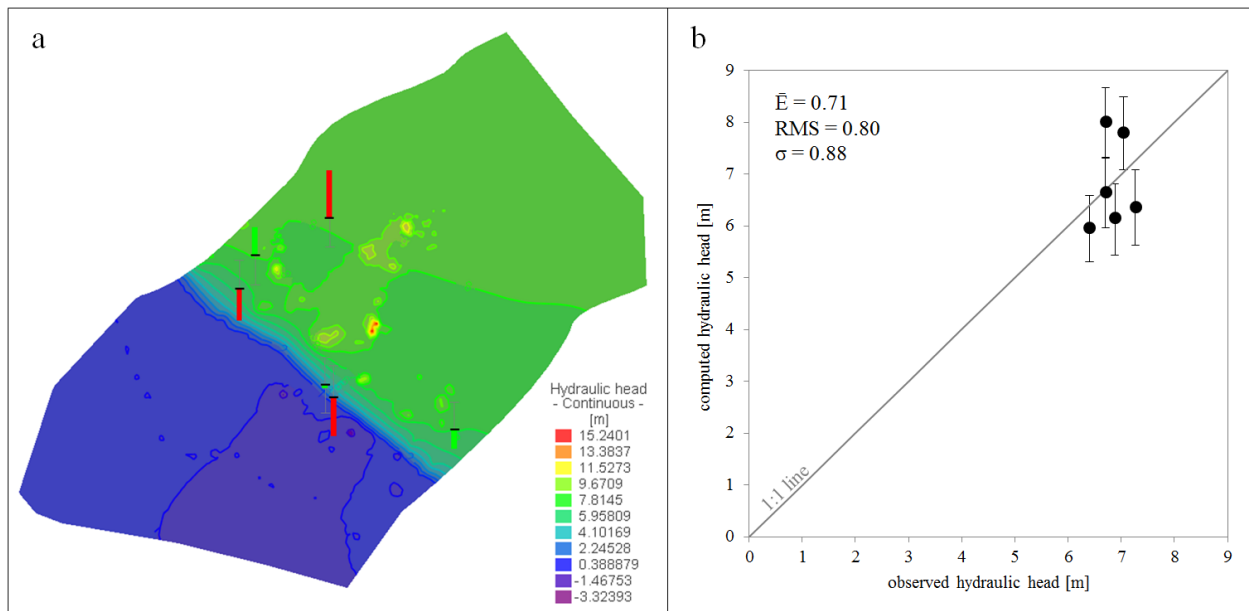


Figure 6. Results of saturated model calibration. (a) Computed head levels under saturated conditions. Green bars indicate when a computed head level fell within a 10% difference from observed head levels. Red bars indicate when a computed head level was greater than a 10% difference from observed head levels. (b) Comparison of observed vs computed head levels. Error bars indicate the 10% interval difference.

4.1.2. Transient saturated flow calibration

The model was further calibrated with transient data from 2004 to 2014. The final head simulation of the previously calibrated saturated, steady-state model was used as the initial conditions for the transient calibration. Transient monthly recharge rates, monthly pumping rates, and observed head levels replaced the steady-state data. All of the original material parameters such as hydraulic conductivity and conductance were kept the same, and specific yield values were included in the transient model. Two scenarios were tested with varying specific yield values. Scenario one had lower Koolau basalt and alluvium specific yield values compared to the scenario two specific yield values. Scenario one resulted in relatively large fluctuations between the observed and simulated head elevations (Fig. 7). Root mean square (RMS) errors were calculated between the observed and simulated head elevations at all three wells. RMS errors at Thomas Square well (1851-02), Kalihi pump station (1952-06-08), and Kapalama T69 well (2052-10) were 1.61, 1.39 and 2.41, respectively. At all three wells, maximum simulated head elevations were higher than the validated levels and minimum simulated head elevations were lower. The results appear to match the average transient head elevations, which is to be expected since the steady-state model was initially calibrated with average recharge and pumping rates. At the Thomas Square well, the simulated transient head elevation was higher than the observed head from 2004 to 2009 (simulation days 0 to 2000), but was then lower than the observed head from 2009 to 2014 (simulation days 2000 to 4000). This same pattern was also seen at the Kalihi pump station. At the Kapalama T69 well, the simulated head was higher than the observed head throughout the entire simulation, but as the simulation progressed, the difference between the observed and simulated heads decreased. The drastic rise and decline in recharge volume around mid-2006 (around simulation day 1000) seems to have the strongest effect on the model. The simulated head elevations follow a steep negative slope while the observed head elevations increase.

Scenario two produced a closer match between simulated and observed head elevations (Fig. 7). RMS errors at Thomas Square well (1851-02), Kalihi pump station (1952-06-08), and Kapalama T69 well (2052-10) were 0.57, 0.45 and 1.65, respectively. All three RMS errors from scenario two are lower than RMS errors from scenario one. Simulated heads generally remained within ± 1 m elevation relative to the observed head elevations for the Thomas Square and Kalihi pump

station wells. Simulated head elevations were still higher than observed heads at the Kapalama T69 well, but were overall closer than the scenario one results. The higher specific yield values allowed for more aquifer drainage, thus producing smaller fluctuations in head as the recharge rates varied over the simulated time span. The smaller specific yield values in scenario one caused the model to withhold the initial flux of recharge added to the aquifer systems, therefore building up head elevations. Thus, the larger specific yield values allowed for a more constant head elevation throughout the aquifer systems over the 11-year simulation time.

There are uncertainties associated with the model calibrations due to the lack of definitive material property values and sensitivity analysis. Different assignments of hydraulic conductivity and specific yield can result in varying calibration results, and since basalt values can range on an order of magnitude, it is not certain what the particular values for these aquifer systems should be. Therefore, the variance seen in Fig. 7 is likely caused by a combination of model uncertainty and a lack of observed data. The degree to which model uncertainty and lack of data contribute to the variance is not quantifiable without sensitivity analysis and formal parameter estimation analyses. Further calibration can provide better results and sensitivity analysis can assist in quantifying the uncertainty of each material property assignment. Such approaches identify parameters of main significance, which is expected to include hydraulic conductivity, and spatial distribution of uncertainty values over the domain. It is also believed that the collection of more observation data that is spatially representative of the modeled area can aid in better calibration. Head elevations, borehole logs, and new drillings can help refine the range of values assigned to the aquifer systems.

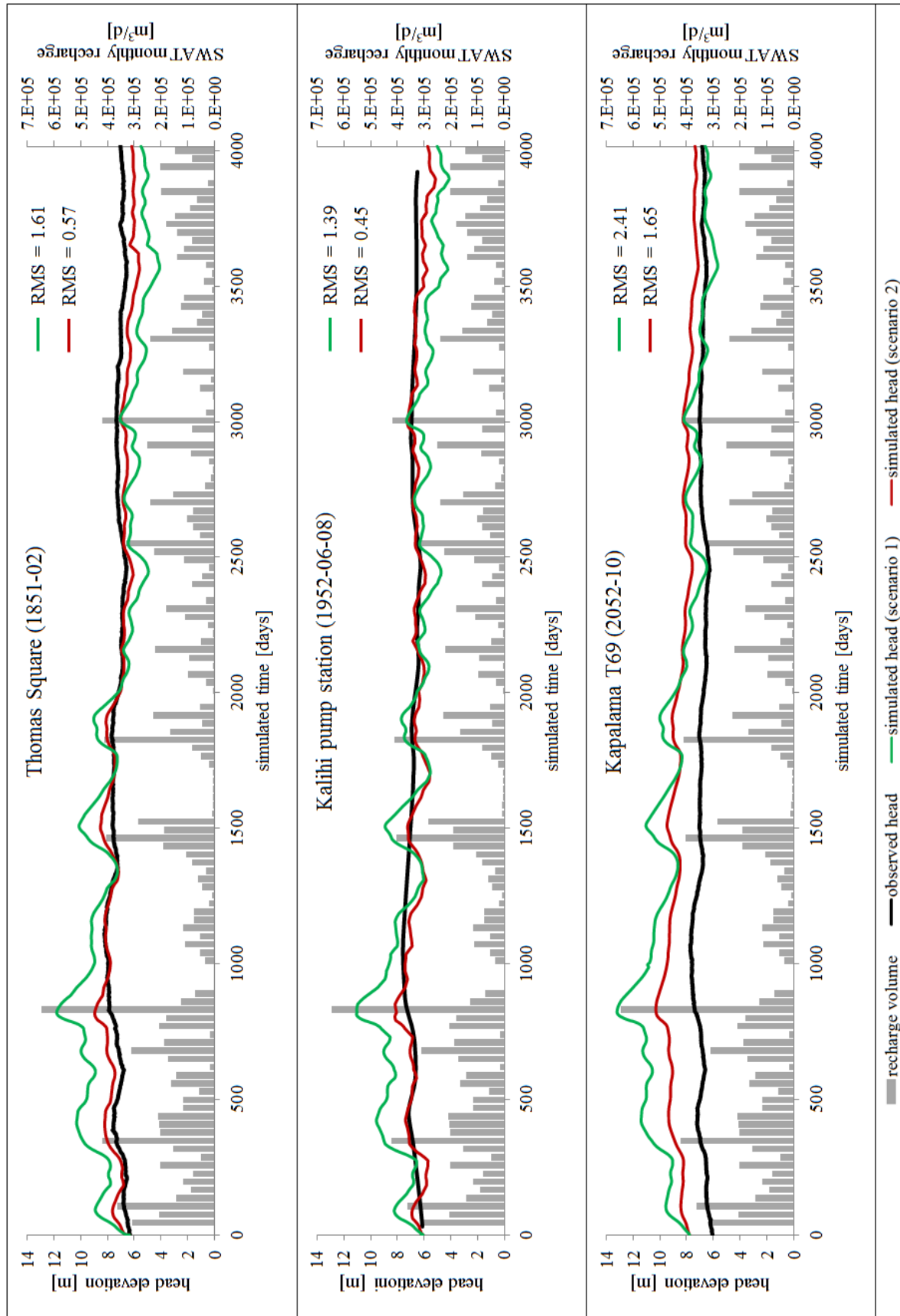


Figure 7. Transient simulated head elevations plotted against transient observed head elevations and transient recharge from 2004 to 2014.

4.1.3. Modeling well injection by use of saturated/unsaturated flow model

The final head simulation of the calibrated saturated, steady-state model (section 4.1.1.) was again used as the initial condition for the saturated/unsaturated model. The calibration results from the saturated flow model were used to extend the modeling to include the unsaturated conditions where the injection well will be located. The model allowed for the assessment of the response of the unsaturated zone of the aquifer to the injected water. The van Genuchten parameters, n and α , were required for the model. Based on calculated van Genuchten parameters for basalt from Magnuson (1995), α was set to 3.8 (1/m) and n was set to 1.4 (dimensionless). Saturated water content (θ_s) was assumed to equal porosity, while the residual value (θ_r) was taken as 0.0025. Dispersivity values were taken as uniform at 20 m and 5 m for the horizontal longitudinal dispersivity and transverse dispersivity values, respectively. There is uncertainty about such values and it is likely that values can vary for different geological materials. By utilizing the final head simulation of the calibrated saturated, steady-state model as the initial condition, the initial moisture content for the saturated zone below the water table was approximately 0.3 (dimensionless) and the initial moisture content for the unsaturated zone above the water table was approximately 0.0009 (dimensionless). The injection well was placed within the forested area next to NR1 (Fig. 8).

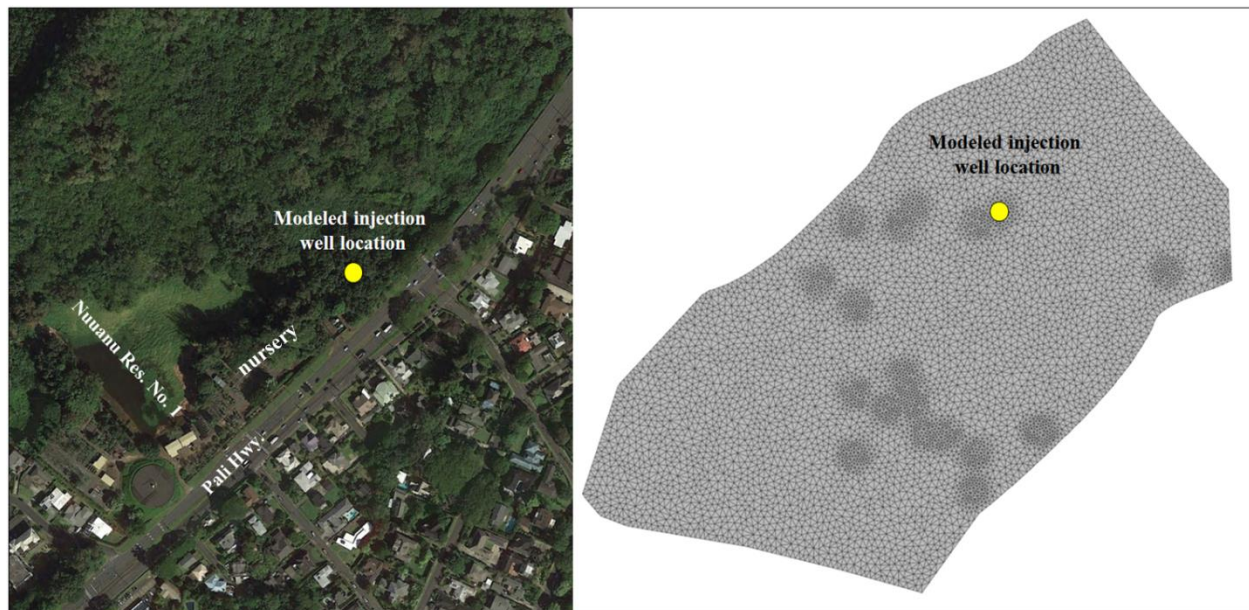


Figure 8. Location of potential injection well against a Google Earth image (left) and the modeled mesh (right). Note: yellow dots are not proportional to scale.

Water cannot be injected into the Koolau basalt considering that the Honolulu volcanics and alluvium layers extend below the current water table. Therefore, the injection well was initially placed at an elevation between 45 and 50 m, which is approximately 75 m below the ground surface and approximately 40 m above the water table. Thus, the injection well falls within the Honolulu volcanics and alluvium as logs suggest (Fig. 9). There is however, high heterogeneity in the geology of the area and without further investigation, it is impossible to accurately identify which layer would be present at that depth. The maximum potential injection rate of 8,631 m³/d was modeled, assuming that the aquifer will most drastically respond to a larger influx.

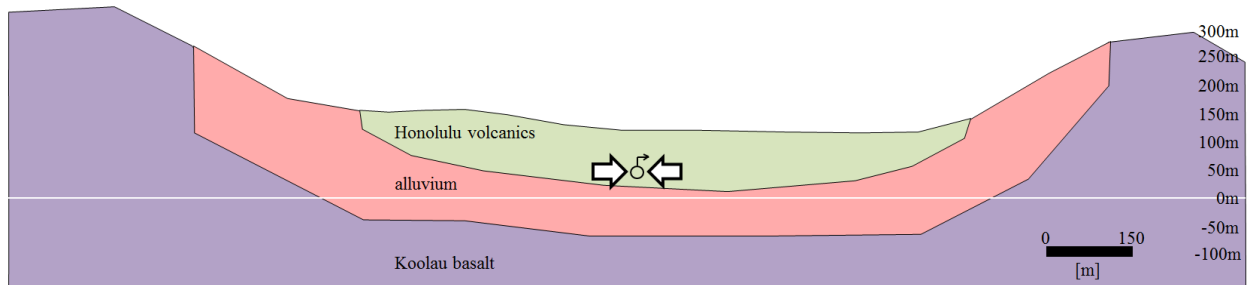


Figure 9. Geologic cross-section through potential injection site. Modeled injection point falls between 45 and 50 m elevation, within Honolulu volcanics and alluvium.

Over the span of 10 years, the water table has the potential to rise approximately 70 m around the injection site (Fig. 10). The simulation predicts that ground flooding due to injection will not occur at this time, but by injecting the maximum potential water under these conditions, the area surrounding the injection well will become fully saturated above the water table. This may violate regulation policies, where the harvested water must be injected into the unsaturated zone of the aquifer system. To avoid this from happening, it is suggested to inject the water at a lower rate and/or inject the water through multiple wells in order to distribute the water across a larger area.

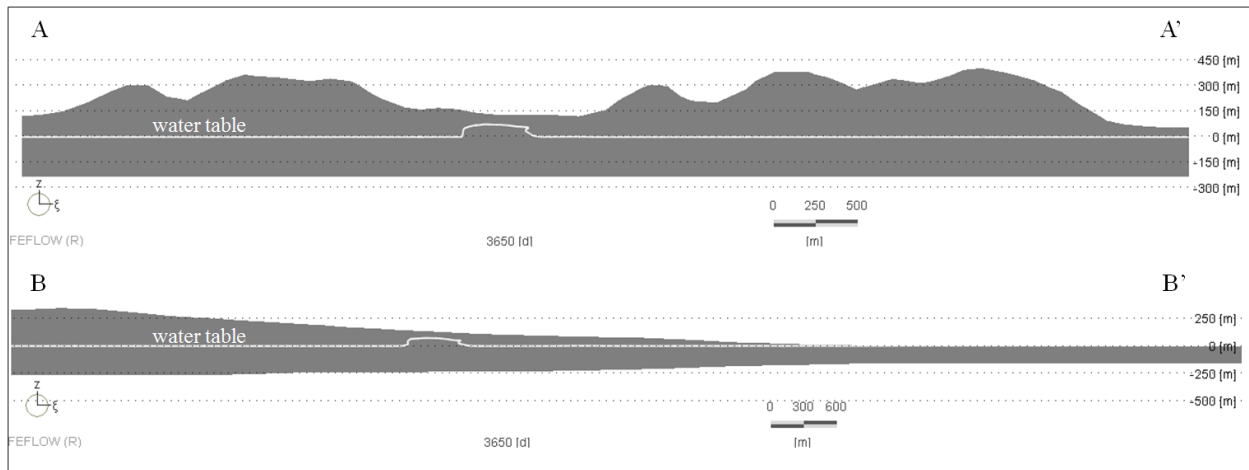


Figure 10. Water table elevation along cross-sections A-A' and B-B' after 10 years of water injection simulation (cross-section lines displayed in Fig. 12, intersecting at the injection point).

A second scenario was simulated to assess how the rate of injection and depth of the injection well affects the moisture content surrounding the injection point. In this scenario, the injection well was placed at an elevation between 80 and 100 m and the injection rate was reduced to $4,315 \text{ m}^3/\text{d}$, which is half of the maximum potential injection rate (Fig. 11). In this scenario, the area directly around the well becomes saturated with the injected water, which is further surrounded by a decrease in moisture content. This indicates that the injected water will be able to reach the saturated zone but will not fully saturate the unsaturated zone to the depth of the saturated zone. Instead, the injected water remains a relatively separate entity, which is allowed to percolate to the saturated zone. There is still a potential for the injected water body to connect with the saturated zone, as seen in Fig. 11, but it does not fully saturate as simulated in Fig. 10. After 10 years of simulation, the injected water body is relatively separate from the saturated zone, but after 25 years of simulation, it is noticed that the moisture content increases between the injected water body and saturated zone. Special attention must be paid to the injection rate and depth to ensure that the injection well is shallow enough to not fall within the saturated zone but also deep enough so that the injected water does not reach the ground surface. There is also a chance to eliminate the problem of fully saturating the area by distributing the injected amount over a number of injection wells.

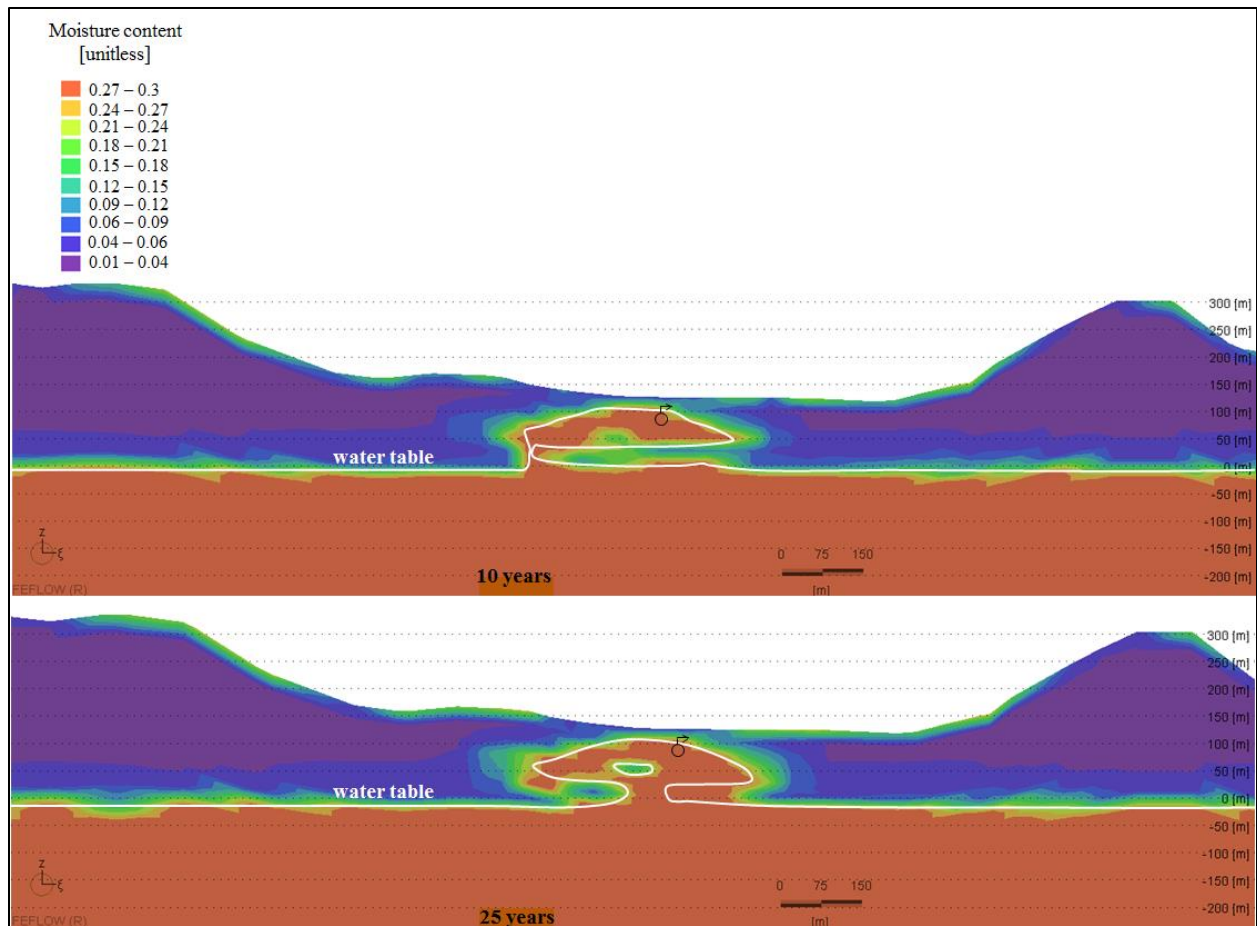


Figure 11. Water table elevation after 10 years (top) and 25 years (bottom) of 4,315 m³/d water injection simulation.

Backwards particle-tracking simulations were used to delineate travel times to the Kalihi pumping station. Capture-zone delineation (CZD) polygons were outlined around the 2-year, 10-year, and 15-year streamlines (Fig. 12). It should be noted that the streamlines are randomly generated and can change in size with different simulated particles. Therefore, the displayed CZD polygons were approximated based on several different CZD simulations. The extent of the simulated pathlines are dependent on the material and storage properties and the random nature of the particle generations. With scenario one porosity values, the injection well falls within the upper edge of the CZD, so some of the injected water should be captured by the Kalihi pumping well within 15 years. With scenario two porosity values, the size of the CZD decreases, therefore the injection well falls outside of the 15-year CZD. Lower porosity values correlate to higher seepage velocities, which allow the water to flow longer distances over shorter time periods.

These CZDs are also smaller in size compared to the SWAP report because of the higher porosity values assigned to the less permeable geologic units. The SWAP report only simulated the basalt aquifer with a porosity of 0.05. Since this model has higher porosity values the overall seepage velocity is lowered, thus requiring more time for the water to flow from the injection well to the Kalihi pumping station.

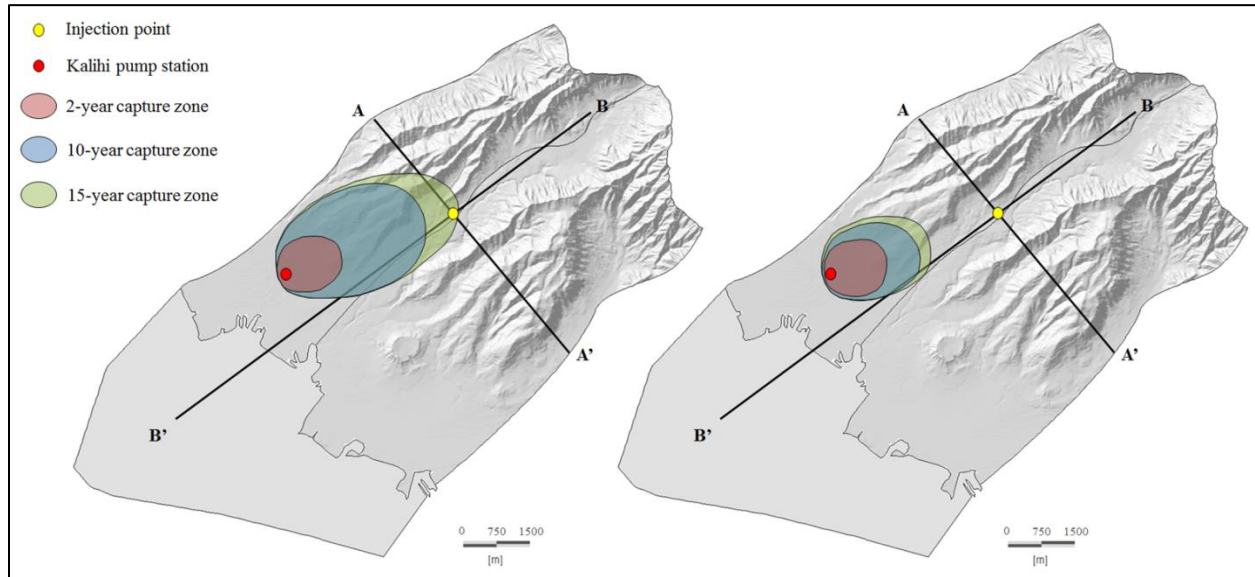


Figure 12. Calculated capture zones of particles reaching Kalihi pump station. Left image created with scenario one porosity values and right image created with scenario two porosity values.

5. SUMMARY AND CONCLUSIONS

The goal of this research was to (1) identify the lithology of Nuuanu and Kalihi aquifer systems and (2) to predict how the aquifers would respond to additional water injection. Borehole logs and surficial geology maps indicate layers of basalt, volcanics and alluvium along the valley floors. It is preferable to inject water into basalt and/or volcanics rather than alluvium because the higher permeability of the volcanic rocks will allow water to infiltrate through the aquifer to reach the saturated zone. The injection process however, should be done in the unsaturated zone between an elevation of 80 to 100 m, where the injection point potentially falls within the Honolulu volcanics. However, there is high heterogeneity in the geology of the area which makes it difficult to accurately identify which layer would be present at that depth.

To predict the response of the aquifers to water injection, three-dimensional, subsurface models were developed for the Nuuanu and Kalihi aquifer systems based on available lithologic and hydrologic data. The model was calibrated under saturated conditions with six observed head levels provided by the USGS, HBWS, and CWRM and further analyzed with transient calibration. The results from the saturated conditions were used to model the injection to be done in the unsaturated zone. The model predicted that the water table elevation will rise around the injection source, but will not greatly impact the overall aquifer by causing groundwater inundation. Since the water will be injected into the Honolulu volcanics and alluvium, the water will require more time to percolate down to the saturated zone, which could be beneficial for filtration or increasing the time of travel to the basal aquifer. Particle-tracking streamlines were computed to delineate the Kalihi pumping station capture zone. The extent of the CZD changes, depending on the porosity values assigned to the aquifer systems. With lower porosity values, the anticipated injection well falls just within the computed 15-year CZD, so the injected water should reach the Kalihi pumping station within 15 years. With higher porosity values however, the anticipated injection well falls outside of the 15-year CZD.

Overall, the Nuuanu and Kalihi aquifer systems should be able to accommodate the additional water injected into Nuuanu Valley, where the injected water and water table is not expected to reach the ground surface. The injection point will most likely need to be in the Honolulu volcanics and alluvium because the Koolau basalt is situated below the water table. The less permeable alluvium will retard the water's immediate vertical movement down into the Koolau basalt, which can allow for a longer filtration time.

The main limitation of this study includes the lack of borehole logs to validate the subsurface lithology. In addition, calibration was hindered by the lack of current observation data across the Nuuanu and Kalihi aquifer systems and lack of extensive calibration data for transient conditions. It is difficult to confidently model the aquifer with only six observed steady-state head levels and three transient head levels, which were not well spatially distributed. It would be desirable to obtain more observation points farther inland to better understand the aquifer's hydraulic gradient. The model also did not simulate possible groundwater flow from adjacent aquifer systems such as Palolo and Moanalua. Geophysical techniques, such as electrical resistivity tomography (ERT), and new borehole logs are recommended to define a more

accurate subsurface characterization. Including the transition zone and underlying saltwater body in a density-dependent model will account for water circulation, which will more accurately simulate the flow of water. Since this model extends past the shoreline, it may not be realistic to apply a no-flow boundary condition to the bottom of the offshore area. A density-dependent model will help to avoid these assumptions made related to the bottom boundary of the model.

Acknowledgements

This project was funded by the Honolulu Board of Water Supply (HBWS) grant C15548001 and I would like to acknowledge DHI for sponsoring the MIKE by DHI student license files. I would like to thank the HBWS staff, Barry Usagawa, Nancy Matsumoto, Kelly Klepinger, Darwina Griffin, Michele Harman, and Kaimana Wong for the support while collecting data and while in the field. I thank Jeremy Kimura from the Department of Land and Natural Resources (DLNR) for his assistance in data compilation. I thank my colleagues and teammates Chris Shuler and Dr. Olkeba Leta for their input and insight. I would finally like to thank my committee, Dr. Aly El-Kadi, Dr. Henrietta Dulai, Dr. Delwyn Oki and Dr. Bradley Carr, for all of their support and guidance. Without their help, this research would not be possible.

References

- Chu, P.-S. and Chen, H., 2005. Interannual and Interdecadal Rainfall Variations in the Hawaiian Islands. *Journal of Climate* (18), 4796-4813. doi: 10.1175/JCLI3578.1.
- Department of Land and Natural Resources (DLNR), 1990. Oahu Water Management Plan. <http://files.hawaii.gov/dlnr/cwrm/planning/wudpoa1990.pdf>
- Diaz, H.F., and Giambelluca, T.W., 2012. Changes in atmospheric circulation patterns associated with high and low rainfall regimes in the Hawaiian Islands region on multiple time scales. *Global Planetary Change* (98-99), 97-108.
- EPA, 2016. Underground Injection Control (UIC): Aquifer Recharge and Aquifer Storage and Recovery: <https://www.epa.gov/uic/aquifer-recharge-and-aquifer-storage-and-recovery> (accessed June 2017).
- Fetter, C.W., 2001. *Applied Hydrogeology*. Prentice Hall, 598 p.
- Finstick, S.A., 1998. Subsurface geology and hydrogeology of downtown Honolulu, with engineering and environmental implications. Water Resources Research Center, University of Hawaii at Manoa.
- Frazier, A.G., and Giambelluca, T.W., 2016. Spatial trend analysis of Hawaiian rainfall from 1920 to 2012. *International Journal of Climatology* (37) 2552-2531. DOI: 10.1002/joc.4862.
- Fredlund, D.G. and Xing, A., 1994. Equations for the soil-water characteristic curve. *Canadian Geotechnical Journal* (31) 521-532.
- Gingerich, S.B. and Oki, D.S., 2000. Groundwater in Hawaii. U.S. Geological Survey Fact Sheet. <https://pubs.usgs.gov/fs/2000/126/pdf/fs126-00.pdf>.
- Habel, S., Fletcher, C.H., Rotzoll, K., El-Kadi, A.I., 2017. Development of a model to simulate groundwater inundation induced by sea-level rise and high tides in Honolulu, Hawaii. *Water Research* (114) 122-134.
- Hunt, C.D., Jr., 1996. *Geohydrology of the Island of Oahu, Hawaii*. U.S. Geological Survey Professional Paper 1412-B.
- Hunt, C.D., Jr., Ewart, C.J., Voss, C.I., 1988. Region 27, Hawaiian Islands *in* *The Geology of North America*. The Geological Society of America (O-2) 255-262.
- Izuka, S.K., Engott, J.A., Bassiouni, M., Johnson, A.G., Miller, L.D., Rotzoll, K., Mair, A., 2016. Volcanic Aquifers of Hawaii – Hydrogeology, Water Budgets, and Conceptual Models. U.S. Geological Survey Scientific Investigations Report 2015-5164. 158 p.

- Kim, Y., Koo, M., Lee, K., Ko, K., Barry, J.M., 2008. Application of analysis and modeling for surface water-groundwater system: preliminary study of artificial recharge in Jeju Island, Korea. AGU Fall Meeting, #H31C-0880.
- Lau, L.S. and Mink, J.F., 2006. Hydrology of the Hawaiian Islands. University of Hawaii Press.
- Leta, O.T., El-Kadi, A.I., Dulai, H., 2017. Implications of Climate Change on Water Budgets and Reservoir Water Harvesting of Nuuanu Area Watersheds, Oahu, Hawaii. Journal of Water Resources Planning and Management (143) 19 p.
- Lucius, J.E., Abraham, J.D., Burton, B.L., 2008. Resistivity profiling for mapping gravel layers that may control contaminant migration at the Amargosa Desert Research Site, Nevada: U.S. Geological Survey Scientific Investigations Report 2008-5091, 30 p.
- Magnuson, S.O., 1995. Inverse Modeling for Field-Scale Hydrologic and Transport Parameters of Fractured Basalt. U.S. Department of Energy, Idaho Operations Office. Report no. INEL-95/0637.
- Martin, R. and Dillion, P., 2002. Aquifer Storage and Recovery: Future Directions for South Australia. Department of Water, Land and Biodiversity Conservation Report 2002/04. http://webdoc.sub.gwdg.de/ebook/serien/ud/DWLBC/DWLBC2002_04.pdf
- Nimmo, J.R., 2009. Vadose Water. Encyclopedia of Inland Waters (1) 766-777.
- NOAA, 2007. Digital Elevation Models (DEMs) for the main 8 Hawaiian Islands. <http://www.soest.hawaii.edu/coasts/data/oahu/dem.html>
- Oki, D.S., 1998. Geohydrology of the Central Oahu, Hawaii, Ground-Water Flow System and Numerical Simulation of the Effects of Additional Pumping. U.S. Geological Survey Water-Resources Investigations Report 97-4276.
- Oki, D.S., 2005. Numerical Simulation of the Effects of Low-Permeability Valley-Fill Barriers and the Redistribution of Ground-Water Withdrawals in the Pearl Harbor Area, Oahu, Hawaii. U.S. Geological Survey Scientific Investigations Report 2005-5253.
- Palmer, H.S., 1946. The geology of the Honolulu ground water supply. Honolulu Board of Water Supply, 55 p.
- Pyne, R.D.G., 2003. Water Quality in Aquifer Storage Recovery (ASR) Wells. American Water Works Association (Florida Section) Annual Meeting. Orlando. <http://asrforum.com/fatestudy/documents/asrpopa111503.pdf>
- RM Towill Corporation, 2013. Final Environmental Assessment: Nuuanu Reservoir No. 4 Repair Project. http://oeqc2.doh.hawaii.gov/EA_EIS_Library/2013-06-23-OA-FEA-Nuuanu-Reservoir-No4-Repair-Project.pdf

- Rotzoll, K. and El-Kadi, A.I., 2007. Numerical Ground-Water Flow Simulation for Red Hill Fuel Storage Facilities, NAVFAC Pacific, Oahu, Hawaii. University of Hawaii & Water Resources Research Center, prepared for TEC Inc., Honolulu, Hawaii.
- Samouëlian, A., Cousin, I., Tabbagh, A., Bruand, A., Richard, G., 2005. Electrical resistivity survey in soil science: a review. *Soil & Tillage Research* (83) 173-193.
- Sherrod, D.R., Sinton, J.M., Watkins, S.E., Brunt, K.M., 2007. Geologic Map of the State of Hawaii: U.S. Geological Survey Open-File Report 2007-1089, 83 p., 8 plates, scales 1:100,000 and 1:250,000, with GIS database.
- Souza, W.R. and Voss, C.I., 1987. Analysis of an anisotropic coastal aquifer system using variable-density flow and solute transport simulation. *Journal of Hydrology* (92) 17-41.
- Stearns, H.T. and Vaksvik, K.N., 1935. Geology and ground-water resources of the Island of Oahu, Hawaii. Hawaii Division of Hydrology, Bulletin 1, 479 p.
- Takasaki, K.J., 1978. Summary Appraisals of the Nation's Ground-Water Resources – Hawaii Region. U.S. Geological Survey Professional Paper 813-M.
<https://pubs.usgs.gov/pp/0813m/report.pdf>
- Timm, O.E., Giambelluca, T.W., Diaz, H.F., 2015. Statistical downscaling of rainfall changes in Hawaii based on the CMIP5 global model projections. *Journal of Geophysical Research: Atmospheres* (120), 92-112, doi: 10.1002/2104JD022059.
- U.S. Census Bureau, 2010 Census Redistricting Data (Public Law 94-171) Summary File, Tables P1 and P2.
<https://factfinder.census.gov/faces/tableservices/jsf/pages/productview.xhtml?src=bkmk>
- van Genuchten, M.Th., 1980. A closed-form equation for predicting the hydraulic conductivity of unsaturated soils. *Soil Science Society of America Journal* (44) 892-898.
- Wentworth, C.K., 1938. Geology and ground-water resources of the Palolo-Waialae District. Honolulu Board of Water Supply, 274 p.
- Wentworth, C.K., 1941. Geology and ground-water resources of the Nuuanu-Pauoa District. Honolulu Board of Water Supply, 218 p.
- Wentworth, C.K., 1951. Geology and ground water resources of the Honolulu-Pearl Harbor Area, Oahu, Hawaii. Honolulu Board of Water Supply, 111 p.
- Whittier, R., Rotzoll, K., Dhal, S., El-Kadi, A.I., Ray, C., and Chang, D., 2010. Groundwater source assessment program for the state of Hawaii, USA: Methodology and example application, *J. Hydrogeology* (18) 711-723.